Characterisation of random DFB Raman laser amplifier for WDM transmission

Characterisation of random DFB Raman laser amplifier for WDM transmission

Paweł Rosa, [1,*] Giuseppe Rizzelli, [1] Mingming Tan, [2] Paul Harper, [2] and Juan Diego Ania-Castañón[1]

[1] *Instituto de Óptica, IO-CSIC, Madrid, 28006, Spain*
[2] *Aston Institute of Photonic Technologies, Aston University, B4 7ET, UK*

[*] *p.g.rosa@icloud.com*

Abstract: We perform a full numerical characterisation of half-open cavity random DFB Raman fibre laser amplifier schemes for WDM transmission in terms of signal power variation, noise and nonlinear impairments, showcasing the excellent potential of this scheme to provide amplification for DWDM transmission with very low gain variation.

OCIS codes: (060.0060) Fiber optics and optical communications; (060.2320) Fiber optics amplifiers and oscillators.

References and links

1. K. Roberts, M. O'Sullivan, K.-T. Wu, H. Sun, A. Awadalla, D. J. Krause, and C. Laperle, "Performance of dual-polarization QPSK for optical transport systems" J. Lightwave Tech. **27**(16), 3546–3559 (2009).
2. J. D. Downie, J. Hurley, D. Pikula, S. Ten, and C. Towery, "Study of EDFA and Raman system transmission reach with 256 Gb/s PM-16QAM signals over three optical fibers with 100 km spans" Opt. Express **21**(14), 17372–17378 (2013).
3. I. D. Phillips, M. Tan, M.F.C. Stephens, M. McCarthy, E. Giacoumidis, S. Sygletos, P. Rosa, S. Fabbri, S. T. Le, T. Kanesan, S. K. Turitsyn, N. J. Doran, and A. D. Ellis, "Exceeding the nonlinear Shannon limit using Raman fibre based amplification and optical phase conjugation" in *Optical Fiber Communication Conference*, OSA Technical Digest, (Optical Society of America 2014), paper M3C.1.
4. M. Tan, P. Rosa, I. D. Phillips, and P. Harper, "Extended reach of 116 Gb/s DP-QPSK transmission using random DFB fiber laser based Raman amplification and bidirectional second-order pumping" in *Optical Fiber Communication Conference*, OSA Technical Digest (Optical Society of America, 2015), paper W4E.1.
5. P. Rosa, J. D. Ania-Castañón, and P. Harper, "Unrepeatered DPSK transmission over 360 km SMF-28 fibre using URFL based amplification" Opt. Express **22**(8), 9687–9692 (2014).
6. P. Rosa, M. Tan, S. T. Le, I. D. Philips, J. D. Ania-Castañón, S. Sygletos, and P. Harper, "Unrepeatered DP-QPSK transmission over 352.8 km SMF using random DFB fiber laser amplification" Phot. Tech. Lett. **27**(11), 1041–1135 (2015).
7. H. A. Fevrier and M. W. Chbat, "Raman amplification technology for bandwidth extension" in *The 14th Annual Meeting of the IEEELasers and Electro-Optics Society* (IEEE, 2001), pp. 344–345.
8. S. B. Papernyi, V.I. Karpov, and W.R.L. Clements "Third-order cascaded Raman amplification" in *Proceedings of Optical Fiber Communication Conference*, OSA Trends in Optics and Photonics (Optical Society of America, 2002), paper FB4.
9. M. Tan, P. Rosa, I. D. Phillips, and P. Harper, "Transmission comparison of ultra-long Raman fibre laser based amplification with first and dual order Raman amplification using 10 × 118 Gbit/s DP-QPSK" in *Proceedings of ICTON*, (IEEE, 2014), paper Tu.C1.7.
10. J. D. Ania-Castañón "Quasi-lossless transmission using second-order Raman amplification and fibre Bragg gratings" Opt. Express **12**(19), 4372–4377 (2004).
11. M. Tan, P. Rosa, S. T. Le, I. D. Phillips, and P. Harper, "Evaluation of 100G DP-QPSK long-haul transmission performance using second order co- pumped Raman laser based amplification" Opt. Express **23**(17), 22181–22189 (2015).
12. S. K. Turitsyn, S. A. Babin, A. E. El-Taher, P. Harper, D. V. Churkin, S. I. Kablukov, J. D. Ania-Castañón, V. Karalekas, E. V. Podivilov "Random distributed feedback fibre laser" Nature Photonics, **4** , 231–235 (2010).
13. P. Rosa, G. Rizzelli, and J. D. Ania-Castañón "Signal power symmetry optimization for optical phase conjugation using Raman amplification" in *Proceedings of Nonlinear Optics*, OSA Technical Digest (online) (Optical Society of America, 2015), paper NW4A.36.

#243952 Received 1 Jul 2015; revised 9 Oct 2015; accepted 11 Oct 2015; published 23 Oct 2015

14. M. Tan, P. Rosa, Md. Iqbal, I. D. Phillips, J. Nuño, J. D. Ania-Castañón, and P. Harper "RIN mitigation in second-order pumped Raman fibre laser based amplification" in *Proceedings of Asia Communications and Photonics Conference*, OSA Technical Digest (Optical Society of America, 2015), paper AM2E.6.
15. J. D. Ania-Castañón,V. Karalekas, P. Harper, and S. K. Turitsyn "Simultaneous spatial and spectral transparency in ultralong fiber lasers" Phys. Rev. Lett. , **101**(12), 123903(1)–(4) (2008).
16. S. Popov, S. Sergeyev, and A. T. Friberg, "The impact of pump polarization on the polarization dependence of the Raman gain due to the breaking of a fibre's circular symmetry" J. Opt. A: Pure Appl. Opt. **6**(3) (2004).
17. M. Alcon-Camas, A. E. El-Taher, J. D. Ania-Castañón, and P. Harper, "Gain bandwidth optimisation and enhancement in ultra-long Raman fibre laser based amplifiers" in *Proceedings of European Conference and Exhibition on Optical Communication* (IEEE, 2010), paper P1.17

1. Introduction

Demand for capacity in the optical communications network is ever growing, driven by the increasing requirements of internet-based technologies. The exponential increase of data traffic over the past decades has driven the development of multiple technologies capable of delivering higher capacities. However, as we approach the physical capacity limits of optical fiber, the need for higher optical-signal-to-noise (OSNR) requirements [1] becomes evident, and the current design of optical networks based on lumped amplification method (EDFA) will not be able to accommodate the less-noise resistant high level modulation formats required to handle the increased capacity needs in a single mode optical fibre [2]. Low noise distributed Raman amplification is now a well-established method that can overcome the limits set by EDFA and satisfy the bandwidth demand. In both long-haul [3, 4] and unrepeatered links [5, 6], it offers a broader bandwidth of operation [7] and improved noise performance compared to lumped amplification [2]. In particular, higher-order pumping can minimise the signal power variation (SPV) and reduce the effective attenuation by pushing the gain farther into the span [8, 9]. Optimised bidirectional Raman pumping can provide the most uniform gain within the transmission span [10] reducing the ASE noise accumulation that results in high received OSNR. However, the unavailability of low RIN high power pumps makes forward pumping in higher order Raman amplifiers problematic due to the high relative intensity noise (RIN) transfer from the noisy Raman laser pumps that counterbalance the benefits of distributed bidirectional amplification in transmission links [11].

A novel amplification scheme that uses a single fibre Bragg grating (FBG) at the end of the transmission span, forming an open cavity with random distributed feedback (DFB) lasing [12] allows for a form of bi-directional pumping that can significantly reduce the growth of amplified spontaneous emmission (ASE) noise [13] without suffering from elevated RIN transfer from the forward pumps [14], becoming an efficient solution capable of extending the transmission distance for coherent data formats [4]. In this paper we characterise the performance and numerically optimise a random DFB Raman laser amplifier for different span lengths, FBG reflectivities and pumps powers. To the best of our knowledge, up to date this is the only experimentally verified high-order, bi-directional Raman configuration that can extend the reach of the coherent transmission beyond backward pumped Raman and EDFA based transmission systems in standard SMF fibre [4], even relying on fibre laser pumps with high inherent RIN.

2. Random DFB Raman laser amplifier

Fig. 1. Schematic design of random DFB Raman laser amplifier.

The schematic design of the random DFB Raman laser amplifier is shown in Fig. 1. To obtain 2nd-order distributed amplification, Raman fibre laser pumps downshifted in wavelength by two

#243952 Received 1 Jul 2015; revised 9 Oct 2015; accepted 11 Oct 2015; published 23 Oct 2015

Stokes shifts with respect to the wavelength of the signal, are placed at each end of the fibre. Instead of creating a closed cavity across the span length with a pair of FBGs, a single FBG centred at 1455 nm with a 200 GHz bandwidth is located at the end of the transmission line to reflect backscattered Rayleigh Stokes-shifted light from the backward pump at 1366 nm and form a random DFB laser acting as a 1st order backward pump that amplifies the signal at 1555 nm. The lack of an FBG on the side of the forward pump significantly reduces the RIN transfer from the forward pump to the Stokes-shifted light at 1455 nm [14] at the cost of a reduction in the power efficiency conversion in comparison to the 1st and 2nd order Raman amplifiers with closed cavities. This is particularly important, as forward-pumping RIN transfer from inherently noisy high-power pumps can seriously degrade data transmission performance [11]. In this configuration, the forward pump at 1366 nm amplifies the backward propagating random DFB lasing at the frequency specified by the wavelength of the FBG.

To simulate each spectral component in wave-division multiplexed (WDM) transmission using random DFB Raman amplification we use an extended model to the one presented in [10, 15], that takes into account residual Raman gain from the primary pump at 1366 nm to the signal in the C-band, pump depletion from both pumps to the lower order pumps and the signal components, double Rayleigh scattering (DRS) and amplified spontaneous emission (ASE) noise for each of the signals, and separates the evolution of noise and signal components at the simulated channel frequencies in order to study the evolution of OSNR, so that the corresponding signal and noise power evolution at frequency ν can be described as:

$$\frac{dP_S(\nu,z)}{dz} = \Bigg(-\alpha(\nu) + g_{R(\mu_2\to\nu)}\left(P_2^+(\mu_2,z)+P_2^-(\mu_2,z)\right) + g_{R(\mu_1,\nu)}\left(P_1^+(\mu_1,z)+P_1^-(\mu_1,z)\right)\Bigg) P_S(\nu,z) \tag{1}$$

$$\begin{aligned}\frac{dn_S^+(\nu,z)}{dz} = & -\alpha_S(\nu)n_S^+(\nu,z)+\varepsilon(\nu)n_S^- \\ & + g_{R(\mu_2\to\nu)}\left(P_2^+(\mu_2,z)+P_2^-(\mu_2,z)\right)\left(n_S^+(\nu,z)+2h\nu\Delta\nu_S\left(1+\frac{1}{e^{\frac{h(\mu_2-\nu)}{K_BT}}-1}\right)\right) \\ & + g_{R(\mu_1\to\nu)}\left(P_1^+(\mu_1,z)+P_1^-(\mu_1,z)\right)\left(n_S^+(\nu,z)+2h\nu\Delta\nu_S\left(1+\frac{1}{e^{\frac{h(\mu_1-\nu)}{K_BT}}-1}\right)\right)\end{aligned} \tag{2}$$

$$\begin{aligned}\frac{dn_S^-(\nu,z)}{dz} = & \alpha_S(\nu)n_S^-(\nu,z)-\varepsilon(\nu)n_S^+ \\ & - g_{R(\mu_2\to\nu)}\left(P_2^+(\mu_2,z)+P_2^-(\mu_2,z)\right)\left(n_S^-(\nu,z)+2h\nu\Delta\nu_S\left(1+\frac{1}{e^{\frac{h(\mu_2-\nu)}{K_BT}}-1}\right)\right) \\ & - g_{R(\mu_1\to\nu)}\left(P_1^+(\mu_1,z)+P_1^-(\mu_1,z)\right)\left(n_S^-(\nu,z)+2h\nu\Delta\nu_S\left(1+\frac{1}{e^{\frac{h(\mu_1-\nu)}{K_BT}}-1}\right)\right)\end{aligned} \tag{3}$$

where P denotes the power of a signal channel or pump, n is the average power of the noise, and $(+)$ and $(-)$ denote propagation in the forward and backward direction, respectively. Subscript S denotes the spectral component corresponds to the wavelength of a signal channel at frequency ν, whereas subscripts 1 and 2 correspond to the primary and secondary pumps at frequencies μ_1 and μ_2 respectively. α represents the attenuation of the fiber at its corresponding frequency, g_R is the effective Raman gain coefficient from frequency μ to frequency ν, ε is the Rayleigh backscattering coefficient, $\Delta\nu$ is the effective bandwidth, h is Plank's constant, K_B is

#243952 Received 1 Jul 2015; revised 9 Oct 2015; accepted 11 Oct 2015; published 23 Oct 2015

Boltzmann's constant and T is the absolute temperature.

Single wavelength pumping may lead to strong Raman polarisation gain dependence in WDM transmission [16]. In this instance, simulations are performed at room temperature with the assumption that Raman pumps at 1366 nm and lasing at the frequency of the FBG are fully depolarised. The noise was calculated in a bandwidth of 0.1 nm. The Raman gain coefficient and attenuation factor for the lasing and each WDM channel was chosen with the respect to the Raman gain spectrum for fully depolarised pumps and attenuation curve in standard SMF silica fibre shown in Fig. 2, respectively. The values of the Rayleigh backscattering coefficients at μ_1, μ_2 and the frequencies of the signals channels are assumed to be 1.0×10^{-4}, 6.5×10^{-5} and 4.5×10^{-5} km^{-1}, respectively.

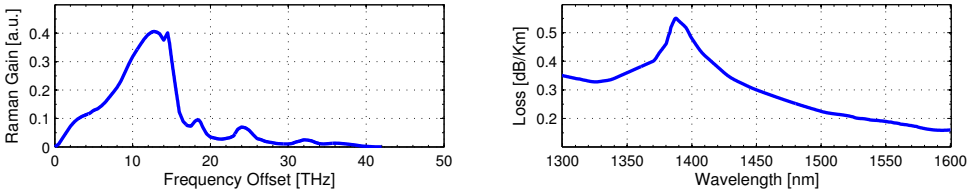

Fig. 2. Normalised Raman gain spectrum (left) and attenuation curve (right) in standard SMF silica fibre used in the simulations.

The simulated average power distribution (0.1 km step) of each component for 100 km single channel transmission (no depletion term) at 1555 nm using random DFB laser amplifier is shown in Fig. 2. The forward and backward pump powers were optimised to give 0 dB net gain at the end of the span. We may notice that the 1455 nm component is dominated by backward propagating lasing (dashed green) that amplifies the signal (solid blue) in C-band region.

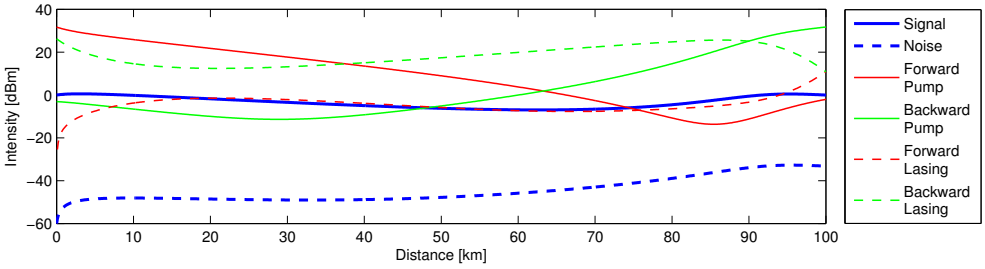

Fig. 3. Numerical simulations of 0 dBm P_s signal (solid blue) at 1555 nm with initial OSNR of 60 dB, forward propagating noise n_S^+ (dashed blue), primary forward pump P_1^+ (solid red), primary backward pump P_1^- (solid green), forward lasing P_2^+ (dashed red) and backward lasing P_2^- (dashed green) power evolution in the 100 km link. In this example forward and backward primary pumps were set to 1.5 W.

3. Results and discussion

3.1. Single channel transmission

The contour plots of the received OSNR, total signal power variation (SPV) and nonlinear phase shift (NPS) in the links from 10 - 120 km are shown in Fig. 4. In the simulations, a single channel at 1555 nm was set to 0 dBm launch power and the forward pump was altered from 0 up to 4 W (with the exception of very short span lengths from 10 to 30 km). The backward pump was set to fully compensate for the span loss and give 0 dB net gain. The SPV was calculated as the difference between the maximum and the minimum power across the transmission span.

The high forward pump power prevents the signal power from dropping at the beginning of the fibre, therefore the received OSNR will increase as expected [Fig. 4(a)], however, most of the signal gain comes from the backward-amplified 1455 nm component [5], hence not much

#243952 Received 1 Jul 2015; revised 9 Oct 2015; accepted 11 Oct 2015; published 23 Oct 2015

RIN is transferred from the forward 1366 nm pump to the signal. A 'sweet spot' for the SPV [Fig. 4(b)] can be found for the forward pump fixed just below 1.5 W. In the simulated fibre length above 90 km, further forward pump power increase gives negligible improvement in the SPV, while increasing the NPS [Fig. 4(c)] significantly, therefore a reasonable trade-off must be applied in the real system design.

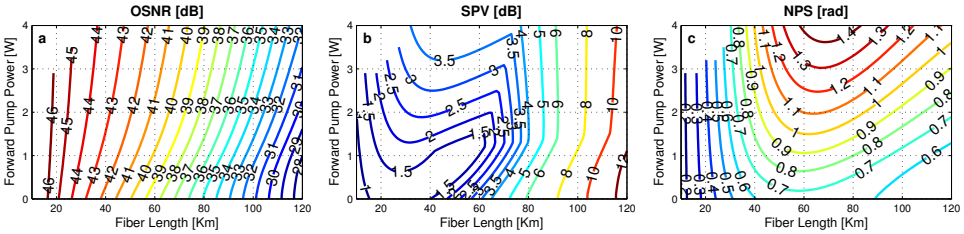

Fig. 4. Contour plots of received OSNR [dB] (a), SPV [dB] (b) and NPS [rad] (c) for the forward pump powers up to 4 W in the links from 10 - 120 km. Backward pump power was simulated to give 0 dB net gain at the end of the span.

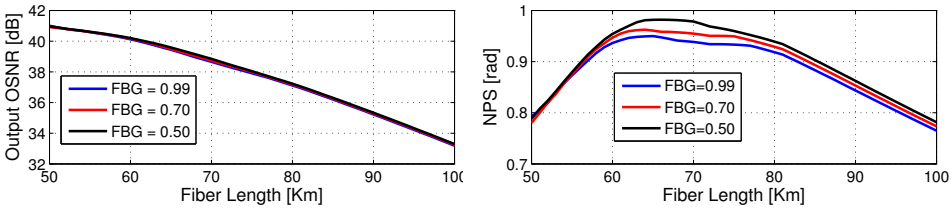

Fig. 5. The impact of the reflectivity of the FBG on received OSNR (left) and NPS (right), measured for the pump power configuration that gives the lowest SPV at the given distance with the realistic forward pump power that is below 1.5 W.

To evaluate the impact of the reflectivity of the FBG at the end of the transmission span, we compare received OSNR and NPS measured at the lowest SPV that gives a reasonable trade-off between the nonlinearity induced degradation due to high forward pumping and accumulated ASE. As we can see from Fig. 4(b) there is a very little improvement in SPV for the forward pump powers above 1.5 W therefore we've chosen best SPV below that level for all distances. This will result in a lower total pump power consumption and more acceptable NPS in the actual data transmission system. Results for FBGs reflectivities of 50%, 70% and 99% are shown in Fig. 5. The received OSNR [Fig. 5(a)] remains the same for all FBGs, however, we may notice an improvement in NPS with the higher FBG's reflectivity [Fig. 5(b)]. Increased reflectivity will also result in better pump power efficiency conversion (reducing the random laser threshold and required pump power).

3.2. Dense WDM transmission

The effect of power transfer from the pump to the signal is an important consideration when designing real WDM transmission systems. Due to pump depletion, the increased number of WDM channels will require higher pump powers. To simulate the impact of the pump depletion on the received OSNR, NPS, SPV and On-Off gain in dense WDM (DWDM) transmission, we fixed forward pump power to 1 W (a reasonable trade-off between OSNR, SPV and NPS shown in Fig. 4) and optimised backward pump for a central channel at 1545 nm to give 0 dB net gain. The number of 25 GHz spaced WDM channels was incremented by 2. The DWDM channel provisioning started in the centre of the C-band at 1545 nm, with subsequent channels being added in pairs either side in the band centre building out towards both ends of the band. The results for the DWDM transmission covering the 1535 - 1555 nm band (up to 100 channels) assisted with the random DFB fibre laser amplifier are shown in Fig. 6.

#243952 Received 1 Jul 2015; revised 9 Oct 2015; accepted 11 Oct 2015; published 23 Oct 2015

The variation in OSNR results from different net gain and SPV (a result of attenuation and Raman gain at a given wavelength). Thanks to combined gain provided by the 1366 nm and 1455 nm pumps, the maximum OSNR difference between the best and the worst performing channels is only about 0.5 dB (0.3 dB on average) in the most loaded case of 100 channels transmission.

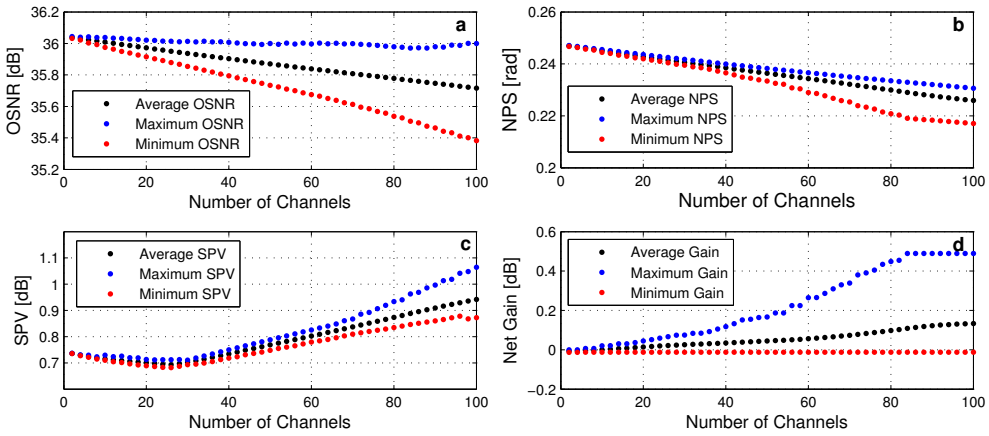

Fig. 6. The performance of the 25 GHz spaced DWDM transmission with up to 100 channels using random DFB Raman laser amplifier. The received OSNR (a), NPS (b), SPV (c) and received net gain (d) are shown for the best (blue) and the worst (red) performing channels. The span length was 50 km and the launch power per channel was set to -5 dBm.

4. Conclusion

The performance of an open-cavity random DFB Raman laser amplification scheme with no grating on the transmitter side for reduced RIN transfer has been numerically studied for DWDM transmission for the first time. Optical signal to noise ratio, nonlinear phase shift, signal power variation, the impact of the reflectivity of FBG and pump depletion have been investigated in standard single-mode fibre from 10 - 120 km. The results show the convenience of using high-reflectivity gratings in this kind of amplifying setup to maximise efficiency without negative impact on performance. The use of high forward pump power ratios improves OSNR performance at lengths above 30 km, but optimal signal power variation is optimised for forward pump powers just below 1.5 W, which could result on a more convenient balance between noise and nonlinearities for systems not limited by ASE. The results show the excellent capacity for the DWDM transmission with total gain variation across the simulated band (1535 - 1555 nm) of less than 0.2 dB on the average. The system might be further optimised by selecting different wavelength of the FBG that would change the overall gain spectrum [17] or applying different optimisation criteria than implemented in this paper (0 dB net gain for a central channel).

Acknowledgments

The authors wish to acknowledge the financial support of the EU through the Marie Skł odowska-Curie IF CHAOS for P. Rosa (658982), FP7 ITN programme ICONE (608099), UK EPSRC programme UNLOC (EP/J017582/1) and the Spanish MINECO TEC-27314 (RAMAS) and SINFOTON (S2013/MIT-2790-SINFOTON-CM). We acknowledge Dr. Javier Nuño for useful discussions.

#243952 Received 1 Jul 2015; revised 9 Oct 2015; accepted 11 Oct 2015; published 23 Oct 2015